Inorganic Chemistry Research

Article

Computational Study of Multiple Pathways and Ion-Pairing in Oxidative Addition of Iodomethane to a Binuclear Organoplatinum(II) Complex containing Imine and Phosphine Bridging Ligands

Allan J. Canty[a,*], Alireza Ariafard[a] and S. Masoud Nabavizadeh[b]

[a]*School o Natural Sciences-Chemistry, University of Tasmania, Private Bag 75, Hobart, Tasmania 7001, Australia*
[b]*Department of Chemistry, College of Sciences, Shiraz University, Shiraz 71454, Iran*

Received: July 29, 2022; Accepted: September 25, 2022
Cite This: *Inorg. Chem. Res.* **2022**, *6*, 93-97. DOI: 10.22036/icr.2022.353871.1133 (Special Issue: In Memory of Prof. Mehdi Rashidi)

Abstract: A density functional theory (DFT) study of the reaction of [$Me_2Pt(\mu$-NN)(μ-dppm)$PtMe_2$] (**1**) (NN = phthalazine, dppm = bis(diphenylphosphino)methane) with two equivalents of iodomethane in acetone (**A**) and benzene (**B**) reveals a mechanism in agreement with spectrocopic and kinetic data reported earlier by Rashidi and coworkers, for which computation permits additional insights. Following initial oxidation at one platinum(II) centre to form mixed valence outer-sphere ion-pairs containing a $Pt^{II}\rightarrow Pt^{IV}$ interaction, [$Me_3Pt^{(+)}(\mu$-NN)(μ-dppm)$PtMe_2{\cdot}I^{(-)}$] (**6A**, **7B**), two competing mechanisms are found for the second oxidative addition at the remaining platinum(II) centre. In one mechanism (Path I), a rearrangement of intermediate **6A** and **7B** to form [$Me_3Pt(K^1$-NN)(μ-dppm)(μ-I)$PtMe_2$] (**2aA**, **2aB**) occurs prior to oxidative addition giving, after subsequent steps, outer-sphere ion-pairs [$Me_3Pt(K^1$-NN)(μ-dppm)(μ-I)$PtMe_3^{(+)}{\cdot}I^{(-)}$] (**10A**, **10B**), followed by dissociation of phthalazine and formation of the product complex [$Me_3Pt(\mu$-dppm)(μ-I)$_2PtMe_3$] (**4A**, **4B**) containing two Pt^{IV} centres.. In the other mechanism (Path 1I), oxidative addition occurs at the Pt^{II} centre of **7A** and **7B**, leading also to **10A** and **10B**. Paths I and II are competitive in acetone, but Path I is preferred in benzene. The first oxidative addition computes as having a lower barrier than the second, in accord with experiment, and we attribute this to the occurrence of a $Pt^a\cdots Pt^b$ interaction assisting the first oxidative addition at Pt^b.

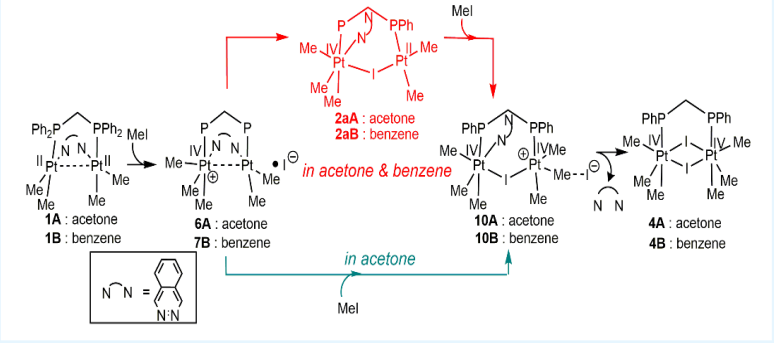

Keywords: Platinum, Oxidative addition, Binuclear complexes, Ion-pairs, Reaction mechanisms, Computation, DFT

1. INTRODUCTION

A rich organoplatinum(II,III,IV) chemistry based on the binuclear manifold "$Pt(L)_2Pt$", has been developed in recent decades,[1] often employing reagents such as alkyl halides as two-electron oxidants. A wide variety of ligands have been utilised, including rigid ligands that ensure separation of platinum centres, and others that allow platinum atoms to be adjacent and participate in Pt···Pt interactions including Pt^{III}-Pt^{III} bonding.

The Rashidi group have made seminal contributions to this field,[2] including computational studies by his colleagues.[3] We report here a computational study of the system illustrated in Scheme 1a, which attracted our attention for several reasons: (i) the potential for a Pt···Pt interaction in an assumed initial cationic intermediate in the reaction of **1** with MeI, (ii) the potential involvement of mixed valence in **2**, **2a**, or other species, noting the assumed flexibility of the weak donor phthalazine bridge and (iii) extensive spectroscopic and kinetic data

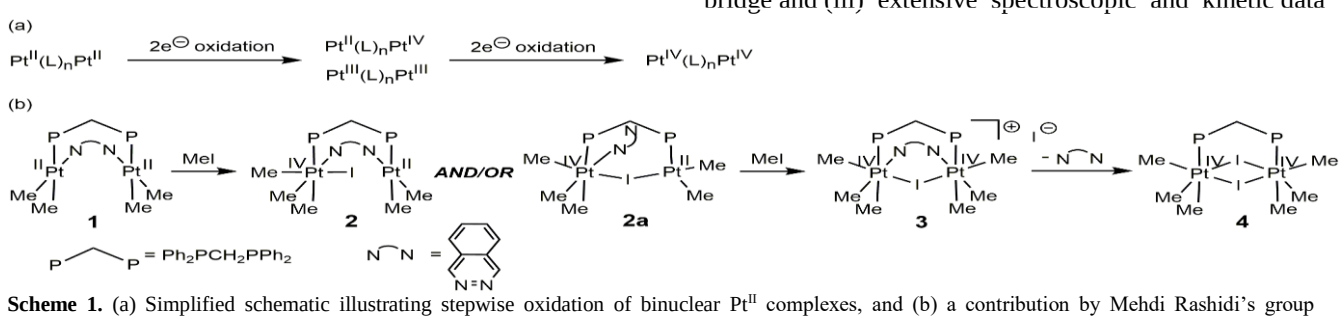

Scheme 1. (a) Simplified schematic illustrating stepwise oxidation of binuclear Pt^{II} complexes, and (b) a contribution by Mehdi Rashidi's group illustrating a proposed mechanism based upon spectroscopic and kinetic data [2a]

available,[2a] including in both acetone and benzene imparting solvent effects on kinetic data, to benchmark mechanisms explored using density functional theory (DFT) methods.

2. RESULTS AND DISCUSSION

First Oxidative Addition in Acetone and Benzene

We commenced this study by examining the first oxidative addition in both acetone (**A**) and benzene (**B**) to allow an initial assessment of complementary experimental and computational data. Optimised structures for the binuclear complex **1** exhibit Pt···Pt 3.450 Å in acetone and 3.476 Å in benzene (**1A** and **1B**, respectively, in Fig. 1), so that this interaction is considered to be very weak (van der Waals radius for Pt 1.73 Å)[4]. Oxidative addition by iodomethane occurs via an initial adduct (**5A**, **5B**) followed by the anticipated S_N2-like transition state (**TS-5A/6A. TS-5B/7B**) leading to products **6A** and **7B** (Fig. 1). During optimisation of **7B** the iodide ion migrated to form an outer-sphere ion-pair in which iodide interacts with *ortho*-hydrogen atoms of phenylphosphine groups linked to the two platinum centres. In contrast, an ion-pair **6A** with a different structure was obtained in acetone, in which the iodide ion interacts with a hydrogen atom of the phthalazine ligand. Reoptimisation of **6A** in benzene also provided **7B**, illustrating a facile rearrangement between ion-pair structures. The Pt···Pt distances decrease on going from **1A**,**B** to **6A** and **7B**, such that the distances in **6A** and **7B** are reduced by ca. 0.5 Å. The shortening reflects the presence of a donor interaction from the Pt^{II} centre to Pt^{IV}, $Pt^{II}\rightarrow Pt^{IV}$, and thus in a formal sense a contribution of Pt^{III}-Pt^{III} bonding.

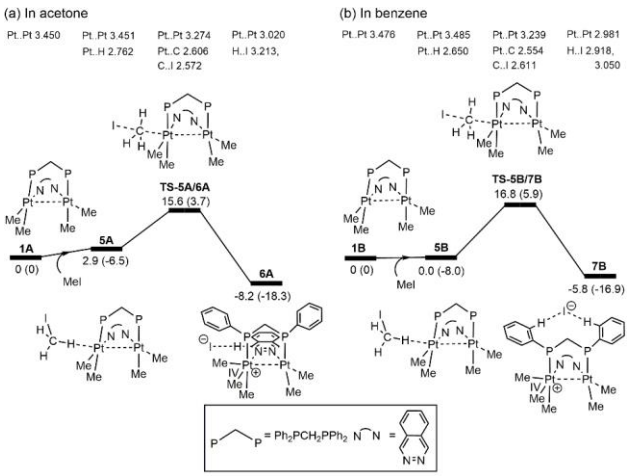

Fig. 1. Computed energy profile for oxidative addition of iodomethane to the binuclear platinum(II) complex [$Me_2Pt(\mu$-NN)(μ-dppm)$PtMe_2$] (**1**) in acetone (a) and benzene (b). The formal oxidation state for "Pt^{IV}" in **6A** and **7B** is shown for simplicity of presentation, noting additional complexity associated with the Pt···Pt interaction. Selected interatomic distances (Å) are shown; energies ΔG (ΔH) are in kcal mol^{-1} referenced to **1A** and **1B.**

The barrier for oxidative addition is computed to be lower in acetone ($\Delta G^{\ddagger}$ 15 6 kcal mol^{-1}) than in benzene ($\Delta G^{\ddagger}$ 16.8 kcal mol^{-1}), consistent with the trend found experimentally ($\Delta G^{\ddagger}$ 17.7 and 18.0 kcal mol^{-1}). The agreement between experimental and computational data provided encouragement for tackling the second oxidative addition.

Second Oxidative Addition in Acetone

Noting the proposed involvement of **2** and/or **2a** (Scheme 1), we explored removal of iodide from the ion-pair **6A** providing **8A**, and adding iodide to the Pt^{IV} centre to give **2A** (Fig. 2a, Path I). The Pt···I distance in **2A** is 3.667 Å, suggesting the presence of a weak interaction. A subsequent process for dissociation of the bridging phthalazine group from the Pt^{II} centre of **2A** to give **2aA** (Fig. 2a) was found from potential energy scans increasing the Pt^{II}-N distance, and subsequent optimisation of a transition state. The barrier for the formation of **2aA**, G 16.6 kcal mol^{-1} relative to **6A**, is higher than the barrier for the initial oxidation (15.6 kcal mol^{-1}, Fig. 1a).

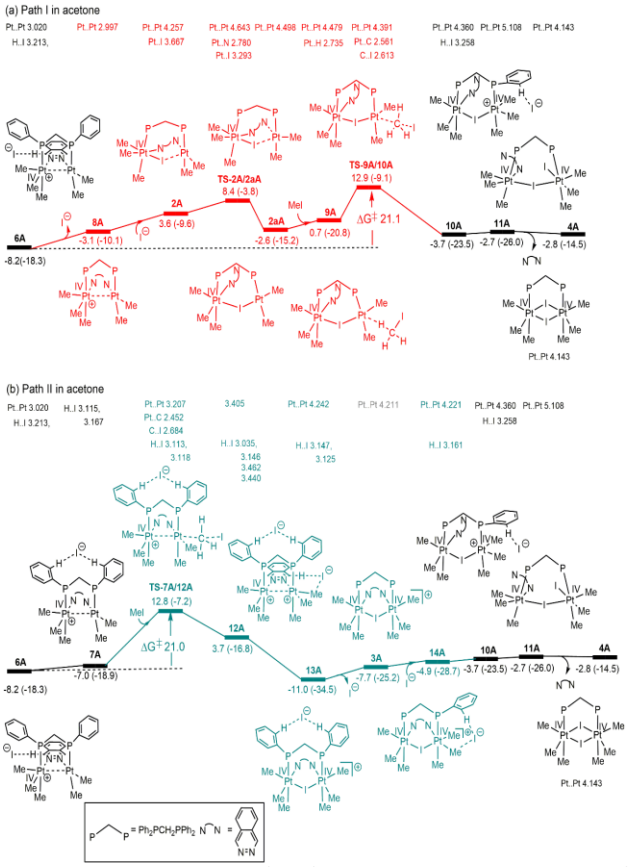

Fig. 2. Computed energy profiles for the second oxidative addition of iodomethane to the binuclear platinum(II) complex [$Me_2Pt(\mu$-NN)(μ-dppm)$PtMe_2$] (**1**) in acetone, commencing from **6A** via (a) Path I and (b) Path II. Selected interatomic distances (Å) are shown; energies ΔG (ΔH) are in kcal mol^{-1} referenced to **1A**.

Oxidative addition occurs readily at the square-planar Pt^{II} centre for **2aA**, via adduct **9A** and **TS-9A/10A**, to give the ion-pair **10A** (Fig. 2a). Coordination of iodide at the square-pyramidal Pt^{IV} centre of **10A** provides **11A**, followed by ring-closure with expulsion of phthalazine resulting in formation of the experimentally isolated complex **4A**.

Path I is consistent with the experimental observation that the second oxidative addition has a higher barrier than the first.[2a]

Path II (Fig. 2b) does not proceed directly from the outer-sphere ion-pair structure **6A**, as a transition state computed for this ion-pair is higher than that found for **TS-7A/12A** ($\Delta\Delta G^{\ddagger}$ 1.8 kcal mol^{-1}). Instead, the process modelled on reaction with the higher energy ion-pair **7A**, as an analogue of the ion-pair formed **7B** formed in benzene (Fig. 1b), provided **TS-7A/12A** and its product (**12A**). Structure **12A** exhibits ion-pair H···I interactions for the iodide ion adjacent to the newly formed Pt^{IV} centre that are ca. 0.2-0.4 Å longer than the iodide ion interacting with the phenylphosphine groups. In a situation where two five-coordinate Pt^{IV} centres are adjacent in **12A**, it is anticipated that the more weakly interacting iodide would migrate to form the lower energy iodo-bridged structure **13A**. Two pathways from **13A** to structure **10A** appear feasible: directly to **10A** via migration of iodide in **13A** to the bridging position, or via dissociation to give **3A** followed by formation of **10A**. Structure **10A** could then form **11A**, allowing completion of reaction as in Path I.

Path I and Path II compute as having identical barriers, and in both cases these barriers are for the oxidative addition step: $\Delta G^{\ddagger}$ 21.1 kcal mol^{-1} for Path I (**TS-9A/10A**) and $\Delta G^{\ddagger}$ 21.0 kcal mol^{-1} for Path II (**TS-7A/12A**) (Fig. 2). It is assumed that reaction can occur via both paths.

Second Oxidative Addition in Benzene

Reaction in benzene was explored in a similar manner to reaction in acetone, resulting in profiles for Path I and Path II that exhibit analogous intermediates and transition states to those for acetone, as shown in Fig. 3. However, for benzene as the solvent, structures directly analogous to fully separated cations and iodide, i.e. analogues of **3A** and **8A** (Fig. 2), compute as very high energy (G 26.2 kcal mol^{-1}) owing to the poor solvation of iodide by benzene, and are thus omitted from Fig. 3.

Except for these differences related to the absence of separated cations and iodide in benzene, the profile for Path I is similar to that in acetone. For Path I and II, the reference point for estimation of the barrier for oxidative addition is **2aB,** as the barrier for interconversion of **2aB** and **6B** ($\Delta G^{\ddagger}$ 13.4 kcal mol^{-1}) is lower than that for the first oxidative addition (16.8 kcal mol^{-1}) and the second oxidative addition (18.1 kcal mol^{-1} for Path I), allowing equilibria between **2aB** and **7B**.

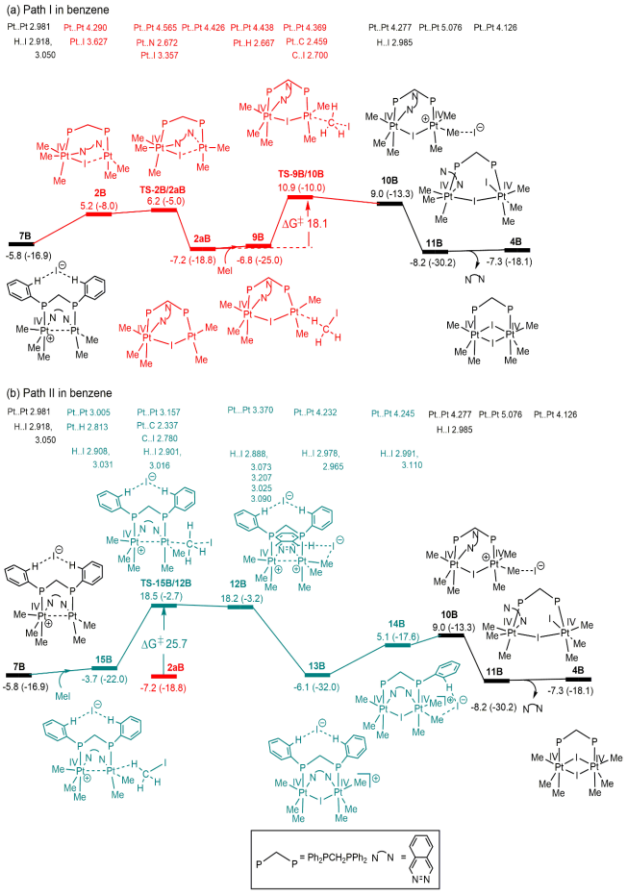

Fig. 3. Computed energy profiles for the second oxidative addition of iodomethane to the binuclear platinum(II) complex [$Me_2Pt(\mu$-NN)(μ-dppm)$PtMe_2$] (**1**) in benzene, commencing from **6B** via (a) Path I and (b) Path II. Selected interatomic distances (Å) are shown; energies ΔG (ΔH) are in kcal mol^{-1} referenced to **1B**.

In contrast with the reaction in acetone, for which Paths I and II are indistinguishable on the basis of $\Delta G^{\ddagger}$, Path II for benzene as solvent is clearly disfavoured ($\Delta\Delta G^{\ddagger}$ 7.6 kcal mol^{-1}). We attribute this to the inability of ion-pairing to compensate for the lower ability of non-polar benzene than acetone to stabilise transition structure **TS-15B/12B** which has adjacent positively charged platinum centres. This aspect is also evident in the product **12B**, which computes as having similar energy to the transition state.

A comparison of experimentally and computationally obtained activation energies is provided in Table 1. For both acetone and benzene, both methods exhibit the first oxidative addition with a lower barrier than the second oxidative addition. Also in agreement, the first oxidative addition has a lower barrier in acetone.

3. CONCLUSIONS

The computational study elaborates in detail the mechanism of the reaction of $Me_2Pt(\mu$-NN)(μ-dppm)$PtMe_2$] (**1**) to form [$Me_3Pt(\mu$-dppm)(μ-I)$PtMe_3$] (**4**)

Table 1. Comparison of Experimental [2a] and Computation Values for Activation Energies for the First and Second Oxidative Addition of Iodomethane to [$Me_2Pt(\mu$-NN)(μ-dppm)$PtMe_2$] (**1**) in Acetone and Benzene

		$\Delta G^{\ddagger}$ (kcal mol^{-1})		$\Delta H^{\ddagger}$ (kcal mol^{-1})	
		Experiment	**Computation**	**Experiment**	**Computation**
First oxidative addition					
	Acetone	17.7	15.6	6.0	3.7
	Benzene	18.0	16.8	8.0	5.9
Second oxidative addition					
	Acetone	18.7	Path I: 21.1 Path II: 21.0	5.3	Path I: 9.2 Path II: 11.1
	Benzene	19.1	Path I: 18.1 Path II: 25.7	10.8	Path I: 8.8 Path II: 16.1

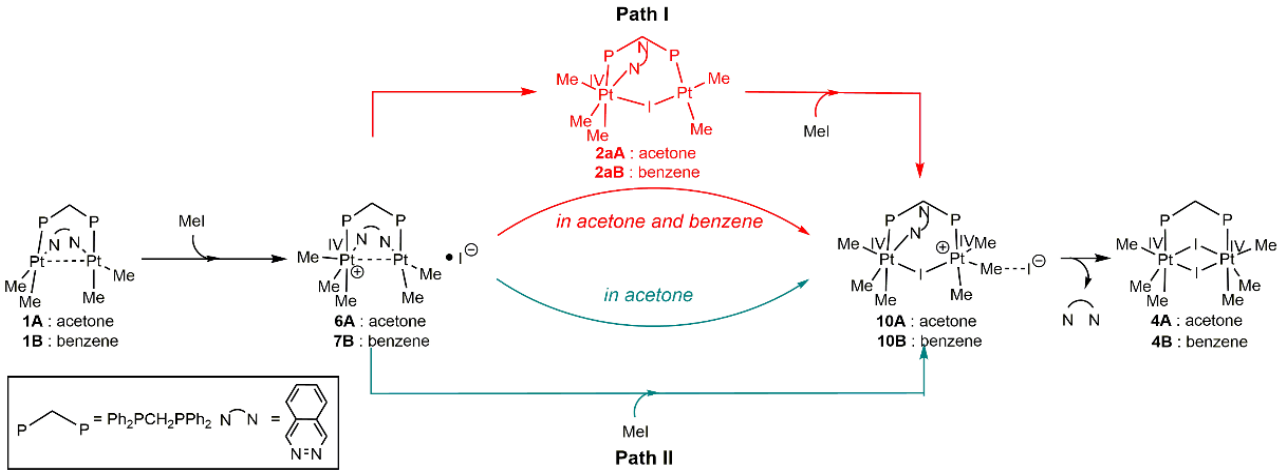

Scheme 2. Computed mechanism for the reaction of **1** with two equivalents of iodomethane to form **4**, illustrating the initial oxidative addition (Fig. 1) and competitive Paths I and II in acetone (Fig. 2), but only Path I in benzene

(Scheme 2) in benzene. The results are broadly consistent with a mechanism proposed on the basis of kinetic and spectroscopic studies (**1** → **2** → **3** → **4**, Scheme 1).

The first oxidative addition forms ion-pairs **6A** (in acetone) and **7B** (in benzene) which exhibit Pt···Pt distances (3.020 Å in acetone, 2.981 Å in benzene), consistent with a weak donor interaction $Pt^{II}\rightarrow Pt^{IV}$. Structures **6A** and **7B** enable entry to two Paths (I and II) for acetone and Path I for benzene, leading to structures **10A** and **10B**, and thus to **4A** and **4B**.

The barriers for oxidative addition in the alternative Paths I and II are essentially identical for acetone as the solvent, so a distinction between these is not considered feasible. These barriers are higher than the barrier for the first oxidative addition, in agreement with experiment.

We attribute the higher barriers for the second oxidative addition as a result of the absence of the presence of a $Pt^{II}\rightarrow Pt^{IV}$ interaction to assist oxidative addition at **2aA** and **7A**, an interaction noted for the first oxidative addition to **1A** and **1B** (Fig. 1).

For benzene as solvent the computed barrier for the first oxidative addition is higher than that for acetone, and the second barrier in benzene is higher than the first, consistent with experiment.

The study indicates the role of a Pt···Pt interaction in the initial oxidative addition, flexibility of the diimine ligand in converting between monodentate and bridging roles, the formation of outer-sphere ion-pairs to stabilise cationic species as key intermediates, the complementary role of experimental (spectroscopy, kinetics) and computation in determining mechanism in organometallic chemistry, and illustrates the important role of Mehdi Rashidi's contribution to modern binuclear organometallic chemistry.

4. EXPERIMENTAL

Gaussian 16 was used[5] to fully optimise all structures at the M06 level of theory.[6] For all the calculations, solvent effects were considered using the SMD solvation model[7] with benzene as the solvent. The SDD basis set[8] *with effective core potential (ECP)* was chosen to describe palladium. The 6-31G(d) basis set was used for other atoms. This basis set combination will be referred to as BS1. Frequency calculations were carried out at the same level of theory as those for the structural optimisation. Computation included application of the ultrafine grid as the default in Gaussian 16. Transition structures were located using the Berny algorithm, contained one imaginary frequency, and exhibited atom displacements consistent with the anticipated reaction pathway. The nature of the transition structures was confirmed from the potential energy surface scans. Transition structures were examined by Intrinsic Reaction Coordinate calculations, and where necessary precursors to and products from transition states were obtained by optimisations after small displacements in

the direction of the normal mode corresponding to the imaginary frequency. To further refine the energies obtained from the SMD/M06/BS1 calculations, we carried out single-point energy calculations in dichloromethane using the M06L functional method[6,9] incorporating Grimme's D3 computation to account more completely for dispersion.[10] for all of the structures with a larger basis set (BS2). BS2 utilises the def2-TZVP basis set[11] on all atoms with an effective core potential including scalar relativistic effect for palladium and iodine. An additional correction for the compression of 1 mol of an ideal gas from 1 atm to the 1 M solution phase standard state (1.89 kcal mol^{-1})[12] was applied.

CONFLICTS OF INTEREST

The authors declare no conflict of interest.

ACKNOWLEDGMENTS

We acknowledge support from the Australian National Computing Infrastructure, University of Tasmania, Iran National Science Foundation and Shiraz University.

AUTHOR INFORMATION

Corresponding Author

Allan J. Canty: Email: allan.canty@utas.edu.au, *ORCID*: 0000-0003-4091-6040

Author(s)

Alireza Ariafard, *ORCID*: 0000-0003-2383-6380.

S. Masoud Nabavizadeh, *ORCID*: 0000-0003-3976-7869.

AUTHOR CONTRIBUTIONS

A. J. C initiated and devised the project, A. J. C and A. A. carried out DFT calculations and contributed to the interpretation of data and writing of the manuscript, and S. M. N. contributed to interpretation of data and writing of the manuscript.

APPENDIX

Electronic Supplementary Information

Supplementary information related to this article can be found at http://doi.org/xxx.

Energy parameters and Cartesian coordinates.

REFERENCES

1. Reviews: (a) K. Matsumoto, M. Ochiai, *Coord. Chem. Rev*. **2004**, *232*, 229. (b) K. Osakada, Comprehensive Organometallic Chemistry III, **2007**, vol. 8, Ch. 8.08. (c) M. Crespo, M. Martinez, S. M. Nabavizadeh, M. Rashidi, *Coord. Chem. Rev*. **2014**, *279*, 115. (d) R. B. Aghakhanpour, S. Pazireh, S. M. Nabavizadeh, S. J. Hosseini, F. Niramood Hosseini, *J. Iran Chem. Soc*. **2020**, *17*, 2683.
2. (a) S. Jamali, S. M. Nabavizadeh, M. Rashidi, *Inorg. Chem*. **2005**, *44*, 8594. (b) S. Jamali, S. M. Nabavizadeh, M. Rashidi, *Inorg. Chem*. **2008**, *47*, 5441. (c) S. J. Hosseini, S. M. Nabavizadeh, S. Jamali, M. Rashidi, *Eur. J. Inorg. Chem*. **2008**, 5099. (d) S. M. Nabavizadeh, H. Molace, E. Haddadi, F. Niroomand Hosseini, S. J. Hoseini, M. M. Abu-Omar, *Dalton. Trans*. **2021**, *50*, 15015.
3. (a) F. N. Hosseini, *Polyhedron*, **2015**, *100*, 67. (b) E. Haddadi, S. M. Nabavizadeh, F. N. Hosseini, *Polyhedron*, **2019**, *164*, 35. (c) R. B. Aghakhanpour, M. Rashidi, F. Niroomand Hosseini, F. Raoof, S. M. Nabavizadeh, *RSC Adv*. **2015**, *5*, 66534.
4. A. Bondi, *J. Phys. Chem*. **1964**, *68*, 441.
5. M. J. Frisch, G. W. Trucks, H. B. Schlegel, G. E. Scuseria, M. A. Robb, J. R. Cheeseman, G. Scalmani, V. Barone, G. A. Petersson, H. Nakatsuji, X. Li, M. Caricato, A. V. Marenich, J. Bloino, B. G. Janesko, R. Gomperts, B. Mennucci, H. P. Hratchian, J. V.Ortiz, A. F. Izmaylov, J. L. Sonnenberg, D. Williams-Young, F. Ding, F. Lipparini, F. Egidi, J. Goings, B. Peng, A. Petrone, T. Henderson, D. Ranasinghe, V. G. Zakrzewski, J. Gao, N. Rega, G. Zheng, W. Liang, M. Hada, M. Ehara, K. Toyota, R. Fukuda, J. Hasegawa, M. Ishida, T. Nakajima, Y. Honda, O. Kitao, H. Nakai, T. Vreven, K. Throssell, J. A. Montgomery, J. E. Peralta, F. Ogliaro, M. J. Bearpark, J. J. Heyd, E. N. Brothers, K. N. Kudin, V. N. Staroverov, T. A. Keith, R. Kobayashi, J. Normand, K. Raghavachari, A. P. Rendell, J. C. Burant, S. S. Iyengar, J. Tomasi, M. Cossi, J. M. Millam, M. Klene, C. Adamo, R. Cammi, J. W. Ochterski, R. L. Martin, K. Morokuma, O. Farkas, J. B. Foresman, D. J. Fox, Gaussian 16, Revision A.03, Gaussian, Inc., Wallingford CT, 2016.
6. (a) Y. Zhao, D. G. Truhlar, *J. Chem. Phys*. **2006**, *125*, 194101. (b) Y. Zhao, D. G. Truhlar, *Acc. Chem. Res*. **2008**, *41*, 157.
7. A. V. Marenich, C. T. Cramer, D. G. Truhlar, *J. Phys. Chem*. B. **2009**, *113*, 6378.
8. A. Bergner, M. Dolg, W. Küchle, H. Stoll, H. Preuß, *Mol. Phys*. **1993**, *80*, 1431.
9. Y. Zhao, D. G. Truhlar, *Theor. Chem. Acc*. **2008**, *120*, 215.
10. (a) S. Ehrlich, J. Moellmann, S. Grimme, *Acc. Chem. Res*. **2013**, *46*, 916. (b) J. Antony, R. Sure, S. Grimme, *Chem. Commun*. **2015**, *51*, 1764.
11. F. Weigend, F. Furche, R. Ahlrichs, *J. Chem. Phys*. **2003**, *119*, 12753.
12. (a) C. P. Kelly, C. J. Cramer, D. G. Truhlar, *J. Phys. Chem. B* **2006**, *110*, 16066. (b) C. P. Kelly, C. J. Cramer, D. G. Truhlar, *J. Phys. Chem. B* **2007**, *111*, 408.